How to Build a Model of the Atmosphere and Spectrum

Robert L. Kurucz

Abstract We want to include the opacity of millions or hundreds of millions of lines in model stellar atmosphere calculations, then generate detailed, realistic spectra from those model atmospheres, then model the observation process, and finally compare the calculated spectra to observed spectra to determine the properties of stars so that we can understand their evolution and the evolution of galaxies.

Keywords Stars: atmospheres · Convection

1 Introduction

Building an LTE, hydrostatic equilibrium model starts by specifying T_{eff}, $\log g$, and abundances. Then you guess a temperature-optical depth relation (using a starting model) for many layers in the photosphere. Then you iterate through the following steps until the flux is constant and temperature is stationary at each layer in the atmosphere:

Compute the equation of state to determine the population of each species and the pressure in each layer.
Compute the line and continuum opacity.
Compute the radiation field and the total radiative flux in each layer.
Compute the convective flux in each layer.
Compute the total flux error and correct the temperature in each layer.

All of this was described in SAO Special Report 309 more than 40 years ago. Some of the coding has not changed since before SR 309 was written about ATLAS5.

R. L. Kurucz (✉)
Harvard-Smithsonian Center for Astrophysics,
60 Garden Street, Cambridge, MA 02138, USA
e-mail: rkurucz@cfa.harvard.edu

E. Niemczura et al. (eds.), *Determination of Atmospheric Parameters of B-, A-, F- and G-Type Stars*, GeoPlanet: Earth and Planetary Sciences,
DOI: 10.1007/978-3-319-06956-2_3, © Springer International Publishing Switzerland 2014

Current versions of ATLAS are much more sophisticated. The report is on my website http://kurucz.harvard.edu/papers as are the previous series of talks I gave in Trieste in 2005:

`/SAO309` ATLAS: A computer program for calculating model stellar atmospheres (Kurucz 1970).
`/triesteatlas12` ATLAS12, SYNTHE, ATLAS9, WIDTH9, etc. (Kurucz 2005a).
`/triestelimits` Physical, numerical, and computational limits for Kurucz codes (Kurucz 2005b).
`/triesterapid` Rapid computation of line opacity in SYNTHE and DFSYNTHE (Kurucz 2005c).
`/triestelines` Including all the lines (Kurucz 2005d).
`/triestesolar` New atlases for solar flux, irradiance, central intensity, and limb (Kurucz 2005e).

Here I will discuss details of topics that are not in textbooks but that affect the accuracy of the results you are able to obtain: observational and computational pipelines, rotation, equation of state, convection and microturbulent velocity.

In Chap. 4 I write about three treatments of opacity and the corresponding programs: Resolved spectra and SYNTHE, Sampled spectra and ATLAS12, Low resolution distribution functions and DFSYNTHE and ATLAS9.

2 Observational and Computational Pipelines

Radiation from a star is affected by a series of interactions before it appears on your terminal screen as a spectrum. These are outlined in the observational pipeline column in Fig. 1. Each interaction can be modelled computationally, although, in practice, some are treated empirically and some are ignored.

3 Rotation

All stars rotate. Except for a tiny percentage that are observed exactly pole-on, the rotation broadens the lines in the spectrum. Observationally the star sends a ray of intensity spectrum toward us from each point on the disk and it Doppler shifts that spectrum by the projected rotation velocity at that point. The total flux spectrum directed at us is the integral over all the rays.

For a slowly rotating, spherical star, computing the flux spectrum is a straightforward process. In ROTATE I tabulate intensity spectra as a function of angle from disk center (limb-darkened spectra). I put a grid over the disk, say 200×200 or 400×400 points, and determine the angle and Doppler shift at each point (Symmetries are taken into account). I interpolate to each grid point, Doppler shift the spectrum, and add it to the integrand for the rotated flux spectrum.

Observational Pipeline	Computatonal Pipeline	Programs
	Grid of models and	ATLAS9/12+
Rotating star	intensity spectra	SYNTHE
	Interp. rotated flux spectrum	ROTATE
Circumstellar material	Circumstellar transmission	not yet
ISM reddening	ISM reddening	REDDEN
ISM lines	ISM lines	not yet
ISM diffuse bands	ISM diffuse bands	not yet
Telluric airglow	Telluric airglow	not yet
Anthropogenic light	Anthropogenic light	not yet
Telluric broad features	Telluric broad features	TRANSYNTHE
Telluric lines	Telluric lines	TRANSYNTHE
Aerosols	Aerosols	not yet
Telescope transmission	From reduction procedure	
Instrumental transmission	From reduction procedure	
Scattered light	From reduction procedure	
Detector sensitivity	From reduction procedure	
Cosmic rays+radioactivity	Removed by red. procedure	
Instrumental profile	From reduction procedure	BROADEN
Observed spectrum	Computed spectrum	
Compare to observed spectrum		PLOTSYN
Iterate		

Fig. 1 Observational and computational pipelines

One complication is that if you look at the Sun with high quality spectra you can actually see differential rotation in the line profiles. Presumably, rapidly-rotating stars have strong differential rotation as well. I have put in an option in ROTATE to compute differential rotational broadening.

The spherical assumption is fine for old, tired stars but young stars are fast rotators, and early type stars can be so fast that they are oblate and have gravity darkening. Figure 2 shows the observed structure of Altair from interferometry by Peterson et al. (2006a). Figure 3 shows Vega determined by Peterson et al. (2006b). Vega looks almost spherical because it is observed almost pole-on. Until recently spectra and the SED (spectral energy distribution) were not determined well enough to show the oblateness and gravity-darkening. The star could be well matched with a simple plane-parallel model, Figs. 4 and 5 (Kurucz 1979). This shows that you can get away with an awful lot if you stick to low resolution.

If we assume that we understand gravity darkening, these stars can be straightforwardly modelled (but we probably do not). As before we place a grid over the star. At each point we determine the angle, the velocity, $T_{\rm eff}$, and $\log g$. We compute a grid of models and spectra covering the whole range of $T_{\rm eff}$ and log g that are possible on the surface. For each model we compute the intensity spectrum as a function of angle. Then we interpolate the spectrum in $T_{\rm eff}$, $\log g$, angle, and Doppler shift at

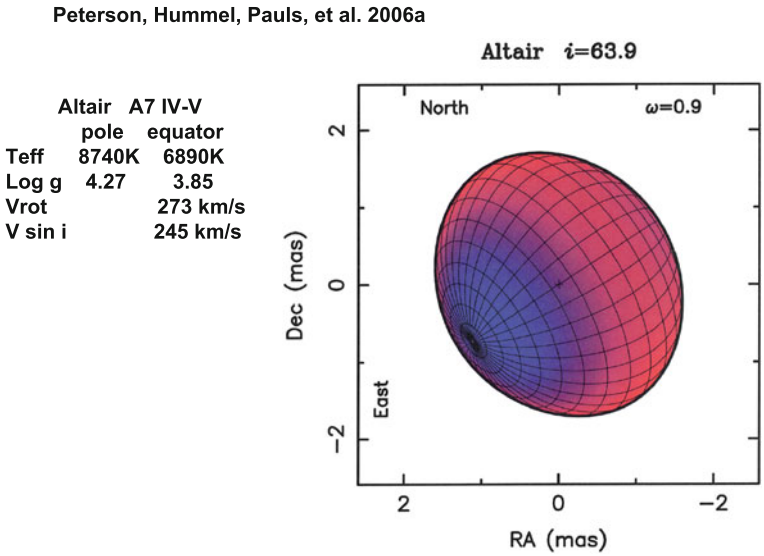

Fig. 2 Altair projected against the sky with derived parameters

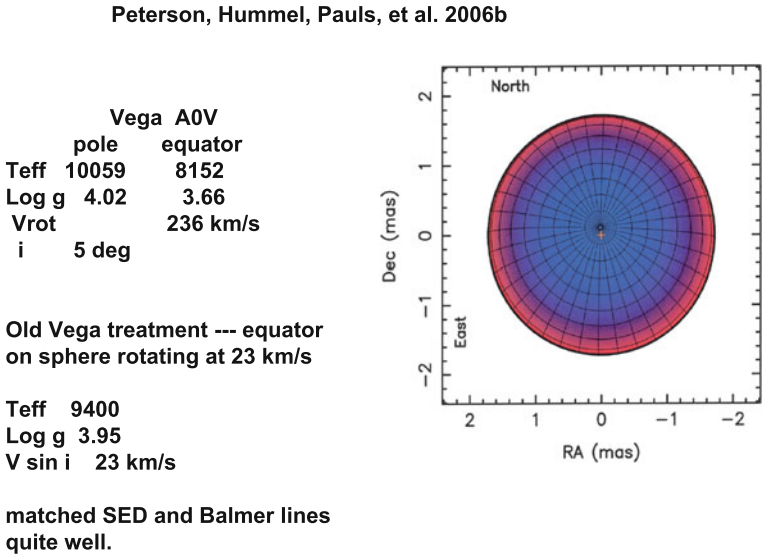

Fig. 3 Vega projected against the sky with derived parameters

each point and add it to the integrand for the rotated flux spectrum. (I am not yet distributing this version of ROTATE).

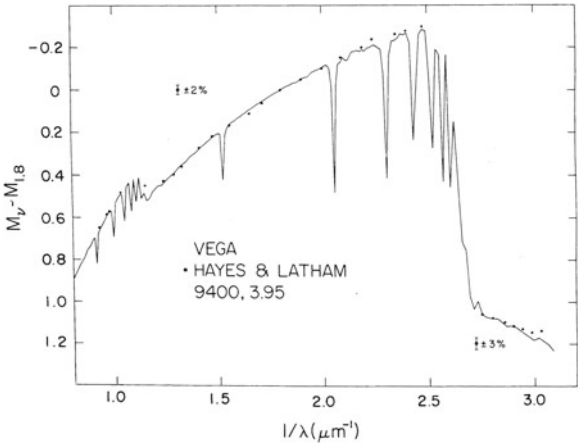

Fig. 4 Old fit to Vega SED from Hayes and Latham (1975) (Kurucz 1979)

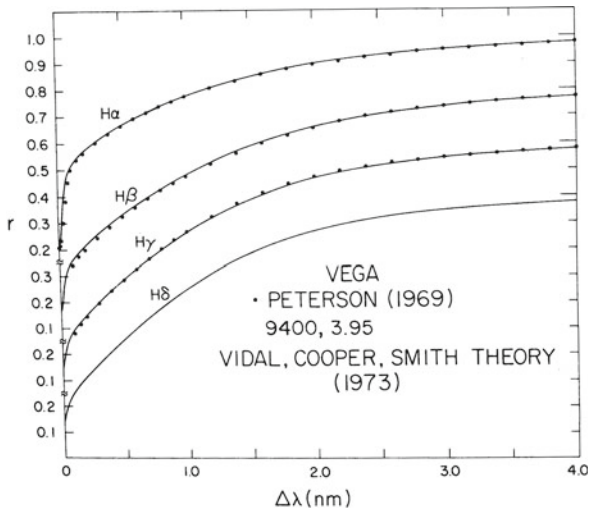

Fig. 5 Old fit to Vega Balmer profiles measured by Peterson (1969) (Kurucz 1979)

4 Circumstellar and Interstellar Absorption

Continuing through the pipeline, Fig. 1:

Circumstellar material: Gas and dust from mass loss, thick disks, zodiacal disks can absorb and produce spectral features and modify the SED.

Interstellar reddening: Program REDDEN reddens SEDs with simple models.

Interstellar diffuse bands: Herbig (1995) has a catalogue of bands.

Interstellar lines: Just search through my line lists for strong lines with lower energies less than 300 cm^{-1}.

These programs are not yet written. Any of you could do it. At present be aware of interstellar features and avoid them.

5 Telluric Spectra

Continuing through the earth's atmosphere:

Telluric airglow: O_2, OH, NO, and other radicals at altitudes above 70 km add emission lines to the spectrum. There are atlases and line catalogues by Osterbrock et al. (2000) and by Cosby et al. (2006), for example. I have not yet programmed it.

Anthropogenic light: There are many city lights in southern Arizona and at other sites that add emission lines to the spectrum. There is a line catalogue by Slanger et al. (2003). I have not yet programmed it.

Any of you could write these programs. In the meantime be aware of the possibility of emission lines.

I have written programs for atmospheric transmission. Given an atmospheric model, which is like a stellar model, temperature and pressure as a function of altitude, program TRANSYNTHE computes the opacity. Then program TRANSPECTR computes the mean transmission from beginning to end of an observation through the atmosphere down to the telescope.

Figure 6 shows absorption by ozone O_3 and O_2 dimer $[O_2]_2$. Figure 7 shows absorption by O_2 and H_2O lines in the visible. Including telluric lines requires very high resolution. I typically use a resolving power of 2 million. That same resolution is then required in computing the stellar spectrum because the spectra are multiplied together point by point by program TRANSMIT. Most of the line data come from the HITRAN line list by Rothman et al. (2005), formerly US Air Force, now Smithsonian Astrophysical Observatory. There is a new edition at http://www.cfa.harvard.edu/hitran. I reformat the HITRAN data into Kurucz format so they can be used as stellar opacity as well.

I have not yet programmed aerosols. They are not significant for residual spectra but matter for absolute spectrophotometry.

6 Comparison to Observed Spectra

Program BROADEN runs the computed spectrum through the measured instrumental profiles. The profile can range from a simple Gaussian to a complicated asymmetric shape with wing structure. (At this stage you can generate spectra at any lower resolution as well, even down to resolving power 100.)

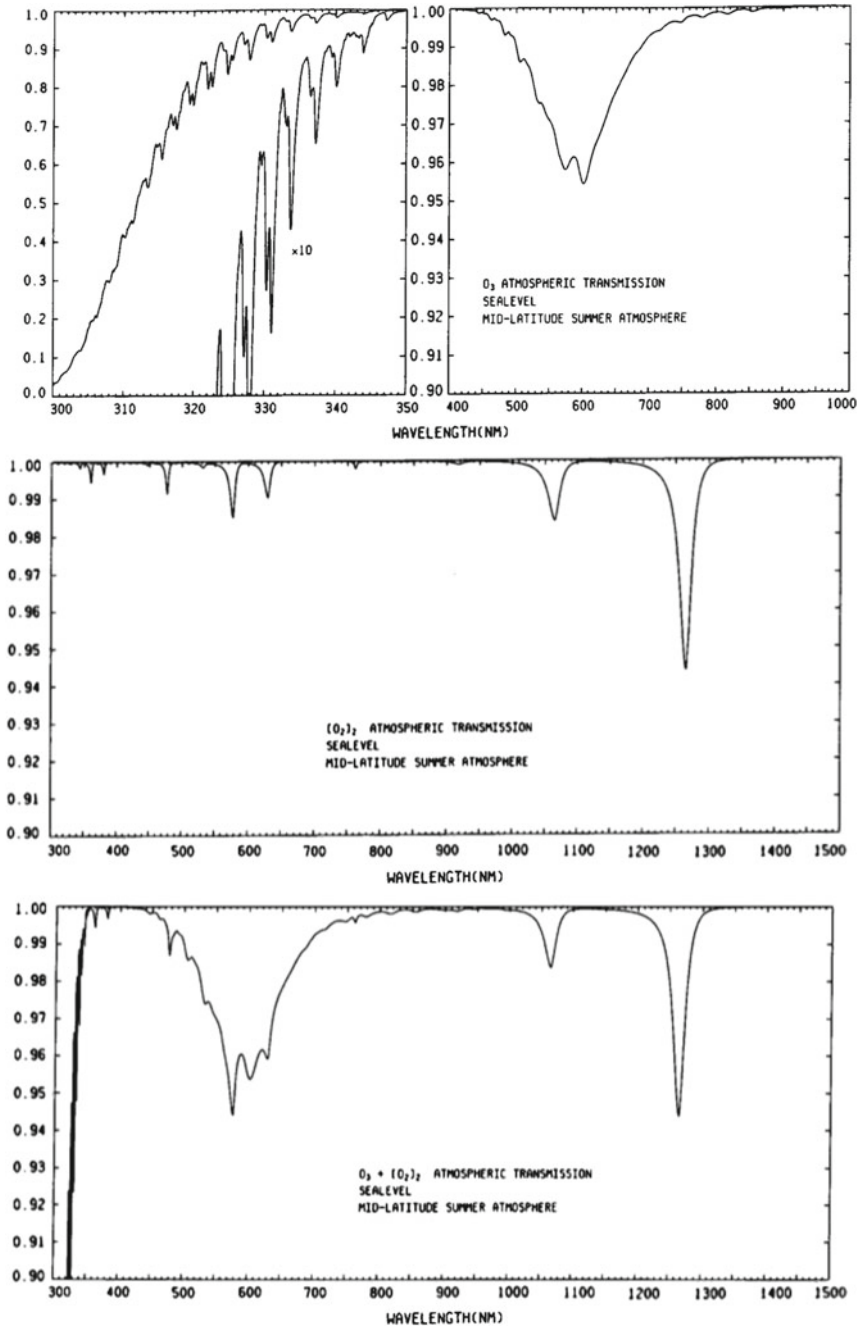

Fig. 6 Atmospheric absorption by ozone and O_2 dimer

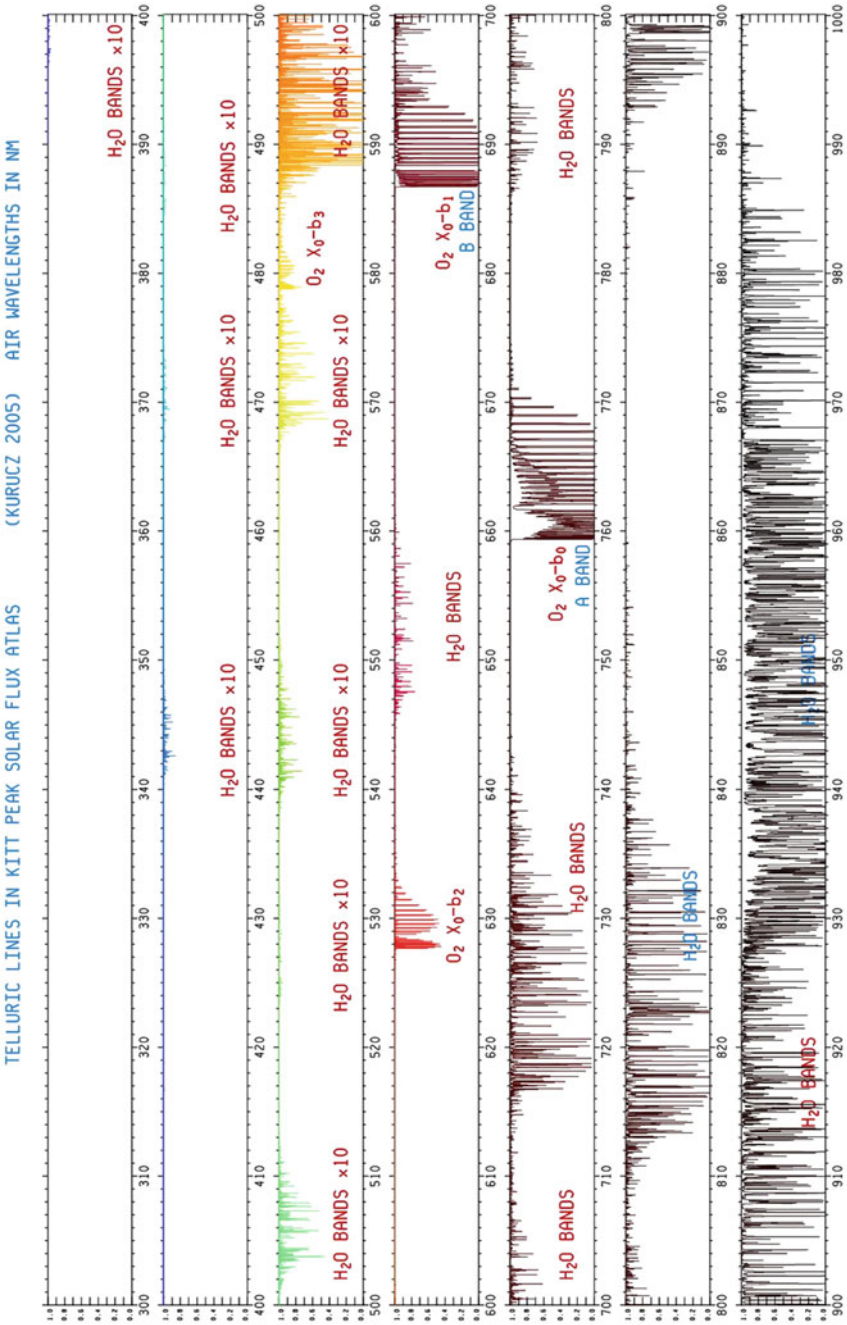

Fig. 7 Telluric lines in Kitt Peak Solar Flux Atlas (Kurucz 2005f)

Then I plot the observed and computed spectra on top of each other with the lines labelled using program PLOTSYN to identify the features and to see what is wrong and what is right. Figure 8 is a Space Telescope spectrum of Sirius at 201 nm. I like it because it illustrates a number of problems.

The observed structures in black are not lines but features that are blends of lines. The 16 km s^{-1} rotation blends the lines together. I have also plotted the spectrum computed with no rotation in blue. This helps indicate the composition of blends.

The minima of the features are not line positions. They frequently fall in between two lines as at 201.1 and 201.41 nm. They cannot be used to set or check a wavelength scale.

Some lines are computed too weak, (201.14 nm); or missing, (201.11 nm); or computed too strong, (201.49 nm).

Figure 9 shows a section of solar spectrum at 599 nm where each spectrum is plotted twice, once at normal scale and once at 10 times scale to show small differences. The observed spectrum is black, the computed solar spectrum is red, the telluric spectrum is blue, and the transmitted spectrum is magenta.

7 Equation of State

All physical data change, hopefully for the better, as time goes by. Even the speed of light has been revised over the lifetime of these programs but is now fixed. Laboratory analyses of atoms and molecules have improved tremendously. There are much more accurate energies and with many more levels known. There are many more lines and with better wavelengths. Partition functions, ionization potentials, and equilibrium constants have changed. I am computing new partition functions and equilibrium constants as I compute new line lists to update the equation of state sections of my programs. You should be aware that the data for ions or molecules that have not been updated can be 30 or 40 years out of date.

8 Convection and Microturbulent Velocity

Figure 10 is the empirical solar model C from Fontenla et al. (1993). The upper darker line is the temperature distribution which drops through the photosphere to the temperature minimum and then rises in the chromosphere. They also determined the microturbulent velocity which drops through the photosphere to a minimum and then rises in the chromosphere. The maximum microturbulent velocity in the photosphere is also the maximum mixing-length convective velocity in my solar model ASUN. I interpret the photospheric microturbulent velocity as convective motions that go to zero in the radial direction toward the surface (Kurucz 1996). Then waves and magnetic motions produce an outwardly increasing chromospheric microturbulent velocity.

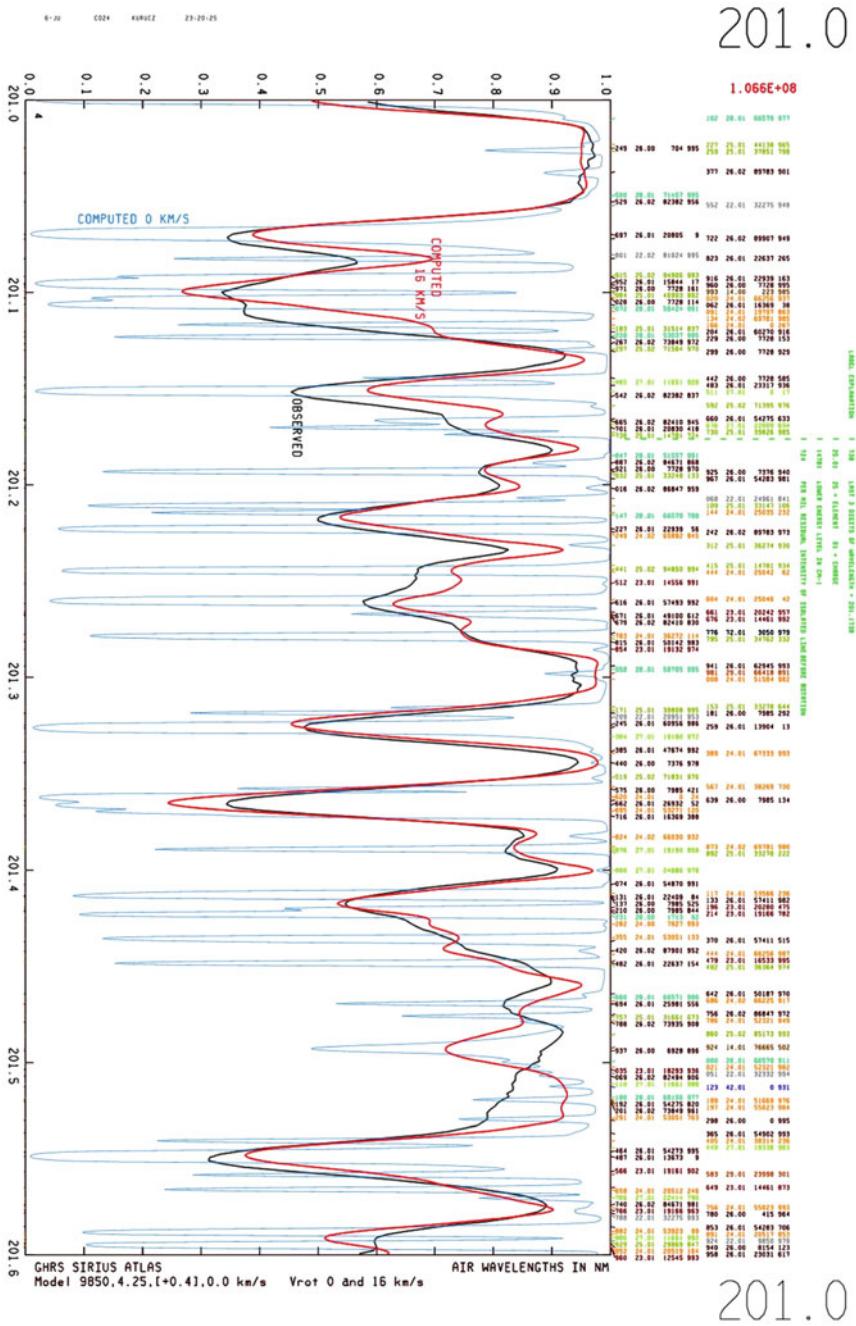

Fig. 8 Comparison of computed and observed Space Telescope GHRS spectra of Sirius

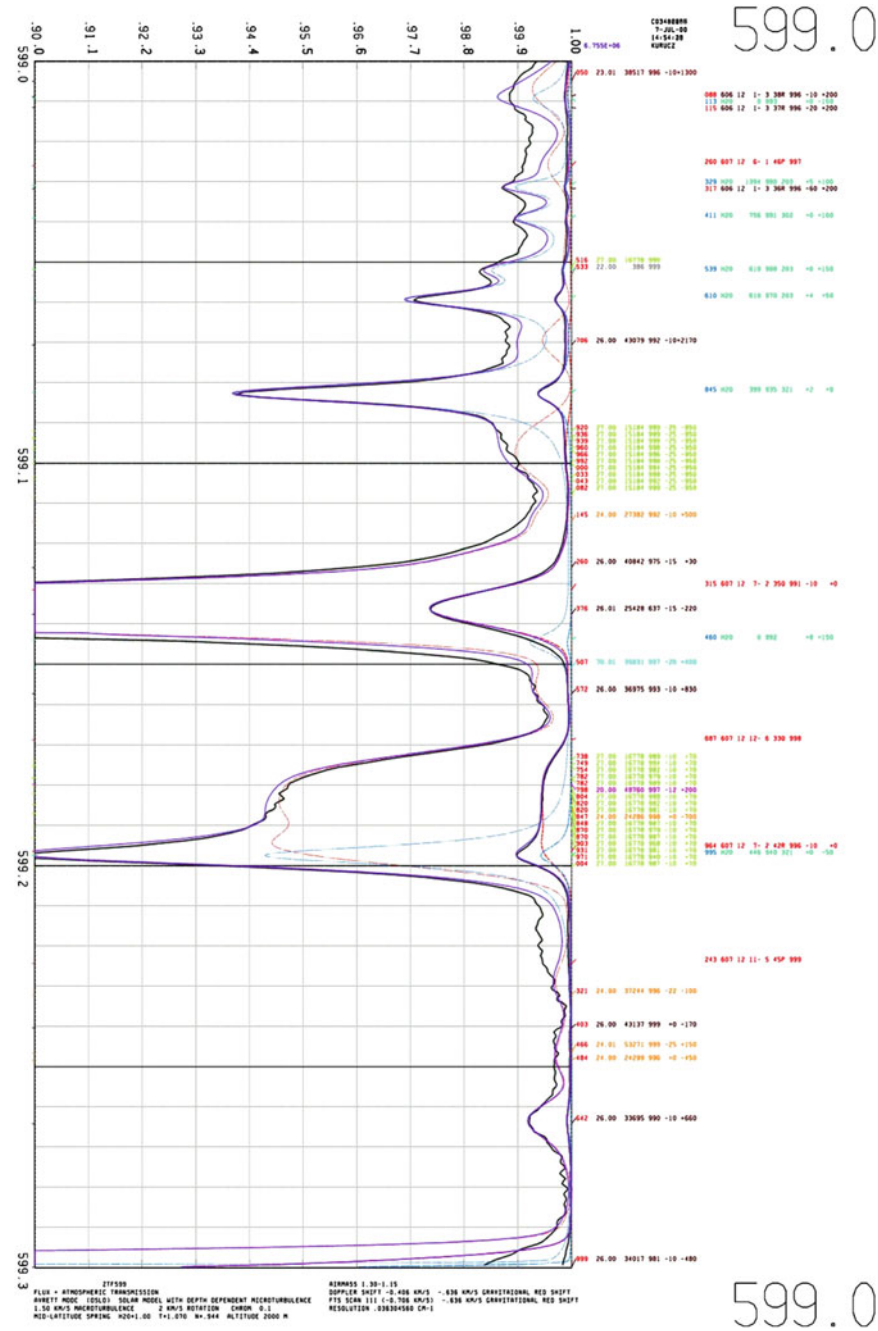

Fig. 9 Comparison of computed and observed Kitt Peak FTS solar spectra

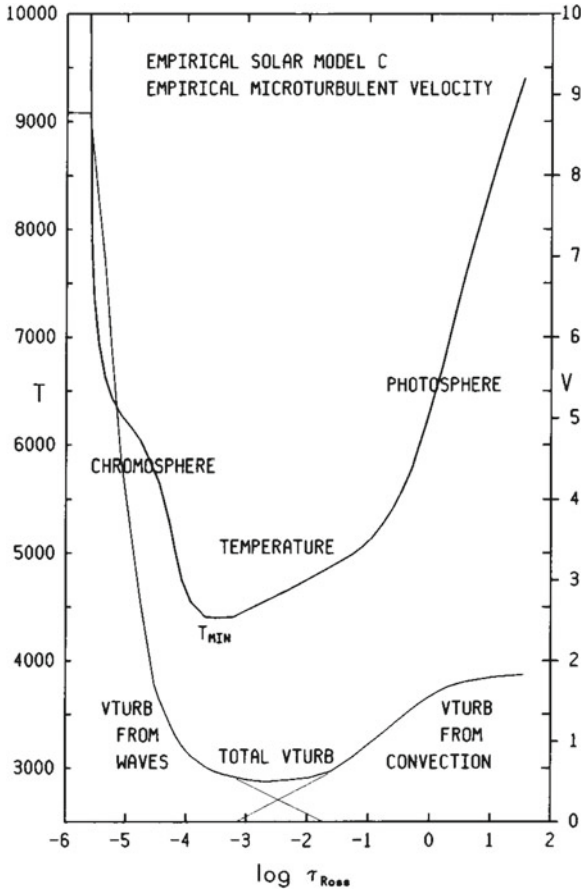

Fig. 10 Empirical temperature and microturbulent velocity distributions in the sun (Fontenla et al. 1993)

I assume that the microturbulent velocity varies the same way in all convective models and I scale the solar profile by the ratio of the maximum convective velocity over a grid of models to the solar maximum convective velocity. The left panel in Fig. 11 shows the maximum convective velocity for a solar abundance grid running from 3,500 to 8,500 K and in $\log g$ from 5.0 down to 0.0. You can see that for a $T_{\rm eff}$ = 3,500 K, $\log g$ = 5.0 M-dwarf the maximum is about 0.25 km s^{-1}; for $T_{\rm eff}$ = 6,000 K, $\log g$ = 4.5 it is about 2 km s^{-1}. You also see that there is a family of smoothly increasing curves as the temperature increases until each curve reaches a maximum and the convection catastrophically falls off and disappears.

The center panel shows the maximum fraction of total flux carried by convection. In the right panel I weight the maximum convective velocities by this fraction and they are the numbers I use to scale the microturbulent velocity.

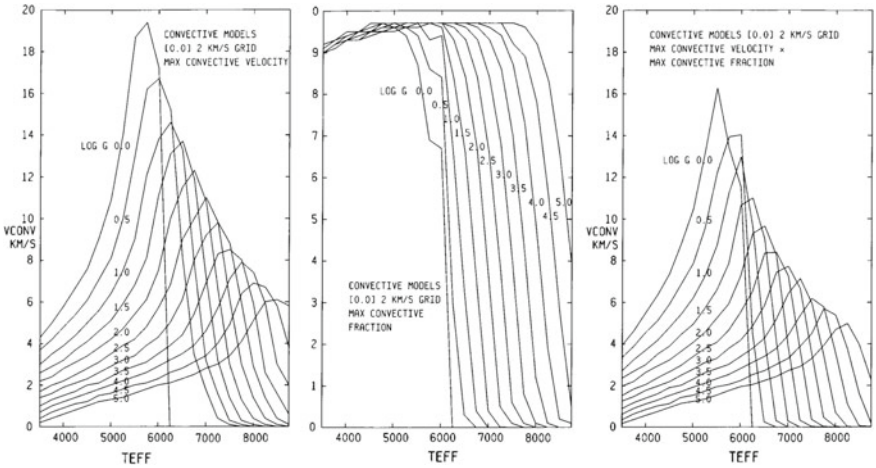

Fig. 11 The maximum convective velocity in a solar abundance grid of models; the maximum convective fraction; the product

At the higher temperatures convective microturbulence decreases and disappears. The microturbulence may actually be zero or other kinds of "microturbulence" may take over. For example, pulsation produces differential velocities that broaden lines.

References

Cosby PC, Sharpee BD, Slanger TG, Huestis DL, Hanuschik RW (2006) J Geophys Res 111:A12307
Fontenla JM, Avrett EH, Loeser R (1993) Astrophys J 406:319
Hayes DS, Latham DW (1975) Astrophys J 197:593
Herbig GH (1995) Ann Rev Astron Astrophys 33:19
Kurucz RL (1970) SAO Spec Rep 309:291
Kurucz RL (1979) Astrophys J Supp 40:1
Kurucz RL (1996) Astron Soc Pacific Conf Ser 108:2
Kurucz RL (2005a) Mem Soc Astron Ital Suppl 8:10
Kurucz RL (2005b) Mem Soc Astron Ital Suppl 8:69
Kurucz RL (2005c) Mem Soc Astron Ital Suppl 8:72
Kurucz RL (2005d) Mem Soc Astron Ital Suppl 8:83
Kurucz RL (2005e) Mem Soc Astron Ital Suppl 8:158
Kurucz RL (2005f) Kitt Peak Solar Flux Atlas (2005f). http://kurucz.harvard.edu/sun/fluxatlas2005
Kurucz RL (2005g) Kitt peak solar irradiance Atlas. http://kurucz.harvard.edu/sun/irradiance2005
Kurucz RL (2008) Irradiance in the H and K bands. http://kurucz.harvard.edu/sun/irradiance2008
Osterbrock DE, Waters RT, Barlow TA, Slanger TG, Cosby PD (2000) PASP 112:733
Peterson DM (1969) SAO Spec Rep 293:199
Peterson DM, Hummel CA, Pauls TA et al (2006a) Nature 440:896–899
Peterson DM, Hummel CA, Pauls TA et al (2006b) Astrophys J 636:1087
Rothman LS et al (2005) JQSRT 96:139
Slanger TG, Cosby PC, Osterbrock DE, Stone RPS, Misch AA (2003) PASP 115:869
Vidal CR, Cooper J, Smith EW (1973) Astroph J Supp 25:37